

THEORETICAL STABILITY PROPERTIES OF A SPACE-CLAMPED AXON

W. KNOX CHANDLER, RICHARD FITZHUGH, *and*
KENNETH S. COLE

*From the National Institutes of Health, Bethesda. Dr. Chandler's present address is
Department of Chemistry, Brown University, Providence.*

ABSTRACT A mathematical method for determining the stability properties of a uniform nerve membrane is developed. Two basically similar tests of stability are considered: examination of the real characteristic roots of the linearized equations and application of a modified Nyquist criterion to the linearized alternating current admittance. The method is applied to the Hodgkin-Huxley equations for the squid axon membrane at 6.3°C to decide theoretically whether stable membrane behavior might be expected in a space clamp experiment. The equations are solved for step depolarizations similar to those used in voltage clamp experiments. Each solution can be represented by a trajectory in the phase space of the variables V , m , h , and n . The stability of motion of a phase point on a given trajectory, and hence the adequacy of the control of the membrane potential, is shown to be a function of the effective conductance in series with the membrane. (For a patch of membrane away from the point controlled by feedback, the effective conductance is the combined conductance of the axial current electrode, axoplasm, and an external layer of sea water, all in series.) In particular, there is a (uniquely determined) critical conductance, defined as the minimum effective series conductance consistent with stability, associated with each point on the trajectory. During a step depolarization the critical conductance goes through a maximum. The values of such maxima as a function of voltage are closely similar to the negative slopes of the peak inward current *versus* voltage curve. This empirical correlation may be helpful in the prediction of stability in experimental situations.

INTRODUCTION

In voltage clamp experiments on the squid giant axon (Cole, 1949; Hodgkin, Huxley, and Katz, 1952; Cole and Moore, 1960), a step change of the measured membrane potential is maintained by electronic feedback. The membrane current required for a cathodal step usually shows (1) an initial capacitative surge, (2) an early, transient current, and (3) a slower, prolonged current.¹

¹ Hodgkin and Huxley (1952) identified the early current as sodium and the slower current as potassium.

However, irregularities in membrane current have been observed during depolarizations of 15 to 50 mv from the resting potential (Frankenhaeuser and Hodgkin, 1957; Tasaki and Bak, 1958; Tasaki and Spyropoulos, 1958; Taylor, Moore, and Cole, 1960). These irregularities arise in parts of the membrane without adequate voltage control and seem to be associated with axial electrodes of high impedance (Tasaki and Spyropoulos, 1958; Taylor, Moore, and Cole, 1960). The appearance of such anomalies raised the question, under what experimental conditions stable control of a nerve membrane might be expected.

A stationary state of a physical system is considered stable if small perturbations from that state do not tend to increase with time. Otherwise it is unstable. For example, a rigid pendulum at rest hanging vertically would be in stable equilibrium, while if rotated 180° it would be in unstable equilibrium. Similarly, a patch of axon membrane is called stable if small perturbations from either a stationary state or a given transient do not tend to increase with time. Otherwise, the patch is called unstable and irregularities in membrane current and voltage can occur. Irregularities can also result from non-uniformities in an axon.

The main purpose of this paper is to present a theoretical analysis of the stability properties of a space-clamped axon, and to show that these depend strongly on the resistance in series with the membrane (primarily axial electrode and axoplasm). The Hodgkin-Huxley equations (Hodgkin and Huxley, 1952) are used for this study mainly because they are the only complete mathematical formulation available for the squid giant axon. However, the analytical methods used in this paper could be applied to other models of the nerve, and similar results are to be expected.

TWO PATCH MODEL

Voltage clamp experiments on squid axons are carried out in this laboratory in the following manner (Cole and Moore, 1960). The potential difference across the membrane is measured between a microelectrode just inside the membrane and a small, external electrode nearby. The difference between a step command voltage and the membrane potential is amplified several hundredfold and applied to a platinized platinum wire, 80-100 μ in diameter, inserted along the nerve axis. Current from this electrode passes through the membrane to a central, external electrode and two lateral guard electrodes. The high gain amplifier delivers the membrane current necessary to maintain the measured potential approximately at the desired clamping potential.

The linear cable model of nerve has been modified to include the shunting effect of the axial wire present in these experiments (Cole and Moore, 1960; Taylor, Moore, and Cole, 1960). The characteristic length for electrotonic spread is a fraction of a millimeter during rest, and slightly less during activity. Thus, the membrane potential a few millimeters from the microelectrode does not appre-

ciably influence the potential measured by the microelectrode. If the longitudinal axoplasm conductance between adjacent areas is ignored, we arrive at the two patch model (Taylor and FitzHugh, 1959; Taylor, Moore, and Cole, 1960) shown in Fig. 1. This model will be used to present the concepts and results of the present study. However, the mathematical methods described and the answers obtained can be applied to more detailed networks.

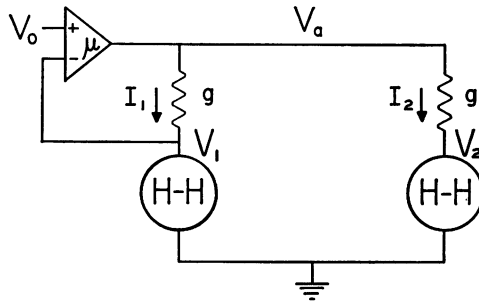


FIGURE 1 The two patch model. The first patch (subscript 1) represents a small, uniform area of membrane at the control point. The second patch (subscript 2) represents an equal area of membrane a few mm away. The conductance g represents axial current electrode, axoplasm, and a small layer of sea water just outside the nerve. The first patch is made electrically stable by the feedback amplifier. The second patch is stable only if g is larger than a certain amount, to be determined.

The patches of membrane are equal in area and sufficiently small that each patch may be considered uniform. The first patch is at the control point; the second patch is more than 2.5 mm away (Cole, 1961). The series conductance g represents the wire surface, axoplasm, and a small layer of sea water around the nerve, all in series. For the present we shall treat g as a dissipative, frequency-independent element. Any resistance between the microelectrode and external electrode in series with the membrane capacity is neglected. A large amplifier gain μ is used to clamp the membrane potential V_1 in the first patch at the command value V_0 . The essential difference between the patches is that random voltage fluctuations in the first patch are controlled by the high gain amplifier, while in the second patch they are not. A small fluctuation arising in the second patch might grow to the extent that the intended voltage course was no longer followed.

In our calculations, the Hodgkin-Huxley equations at 6.3°C are used to represent each patch. The first study of this model was made by Taylor and FitzHugh (1959) with the aid of an analog computer. Their results have been published in detail (Taylor, Moore, and Cole, 1960). Step potentials V_0 were applied to the control amplifier and reproduced by the first patch. The potential V_2 across the second patch also followed V_0 when g was large enough. However, when g was made small V_2 deviated from a step, and notches, similar to those seen experimentally, appeared in the current patterns. When the two series conductances had

different values, a condition used to simulate axon non-uniformity, the potential V_2 across the second patch always deviated from V_1 . The second patch was stable when the values of the conductances were large, and unstable when they were small.

In this paper, we shall consider only the uniform case where each patch has the same series conductance. This has the advantage that the exact mathematical solution of the response of the second patch is the same as for the first patch, while for different conductances each combination would require a separate solution. The disadvantage is that the results are applicable only to spatially uniform axons.

MATHEMATICAL INTRODUCTION

Space will not permit a complete exposition of the mathematical methods used. They are based on standard methods of the theory of nonlinear differential equations, as described in the books of Minorsky (1947), Andronow and Chaikin (1949), Bellman (1953), Lefschetz (1957), Nemytskii and Stepanov (1960), and others. In what follows we will ignore many difficulties of mathematical rigor and apply this theory in what we believe to be an appropriate way to our problem.

The results of this study are most simply expressed in terms of a quantity which we shall call the critical conductance g_c . A series conductance larger than this value is necessary for stability in the second patch, while a smaller conductance can cause instability. The concept of stability will be first applied to the Hodgkin-Huxley equations for a steady state, and then modified to apply to the transient associated with a voltage clamp pulse. During a given step depolarization g_c varies with time, going through a maximum. If the series conductance is larger than this maximum value, the second patch will be stable throughout the pulse. Two complementary methods of calculating g_c , from the characteristic equation and from the Nyquist stability criterion, will be described in the following two sections.

CHARACTERISTIC EQUATION

A mathematical criterion for stability will be first outlined for a general system, and then applied to the Hodgkin-Huxley equations in the two patch model. Consider a physical system represented by a set of simultaneous, first order differential equations of this form

$$dx_i/dt = F_i(x_1, x_2, \dots, x_n) \quad i = 1, 2, \dots, n.$$

The singular or equilibrium points of the system are defined by $dx_i/dt = 0$ for all i . A singular point is stable if, for any small neighborhood in the x phase space enclosing the point, the phase point (x_1, x_2, \dots, x_n) remains indefinitely in the neighborhood when perturbed from the singular point by an amount smaller than a predetermined quantity. Otherwise, a small perturbation might grow, moving the

phase point some distance from the singular point, which, in this case, would be unstable.

To determine whether a singular point is stable or not, the equations are expanded in Taylor's series about the point (Adams, 1957) and the non-linear terms are discarded. The result is

$$d(\delta x_i)/dt = \sum_{j=1}^n m_{ij} \delta x_j \quad i = 1, 2, \dots, n, \quad (1)$$

where $m_{ij} = \partial F_i / \partial x_j$, evaluated at the singular point, and δx_i is the perturbation of x_i from the singular point. Liapunov's theorem (Minorsky, 1947; Lefschetz, 1957) states that (ignoring certain borderline cases) the stability of the singular point $\delta x_i = 0$, for all i , in the linear system represented by equation (1) is the same as the stability of the original singular point in the nonlinear system. A solution of the form

$$\delta x_i = a_i \exp(\lambda t) \quad (2)$$

satisfies equation (1) if

$$(\mathbf{M} - \lambda \mathbf{I})\mathbf{A} = 0, \quad (3)$$

where \mathbf{M} is the coefficient matrix with elements m_{ij} , \mathbf{I} is the identity matrix, and \mathbf{A} is the column vector with elements a_i . A non-trivial solution for \mathbf{A} exists if the determinant

$$|\mathbf{M} - \lambda \mathbf{I}| = 0. \quad (4)$$

This characteristic equation is of n^{th} degree in λ , with n roots, real or complex. *If the real part of each λ satisfying this equation is less than zero, all perturbations δx from the singular point tend to decrease with time, and the singular point is stable. If at least one root has a positive real part, the singular point is unstable.*

We apply this analysis to the Hodgkin-Huxley equations

$$\dot{V} = I/C - \bar{g}_{Na} m^3 h (V - V_{Na})/C - \bar{g}_K n^4 (V - V_K)/C - \bar{g}_L (V - V_L)/C$$

$$\dot{m} = \alpha_m (1 - m) - \beta_m m$$

$$\dot{h} = \alpha_h (1 - h) - \beta_h h$$

$$\dot{n} = \alpha_n (1 - n) - \beta_n n.$$

A dot is used to indicate differentiation with respect to time. The symbols used are those used by Hodgkin and Huxley (1952).

LIST OF SYMBOLS

I = membrane current density, positive outward² ($\mu\text{amp}/\text{cm}^2$)

V = membrane potential as mv deviation from resting potential, depolarization positive²

² The sign convention of I and V is opposite to that used by Hodgkin and Huxley (1952). The α 's and β 's, which are functions of V , have been changed accordingly.

$$g_{N_a} = \bar{g}_{N_a} m^3 h$$

$$g_K = \bar{g}_K n^4$$

$$g_\infty = g_{N_a} + g_K + g_L = \text{infinite frequency membrane conductance}$$

$$\tau_m = 1/(\alpha_m + \beta_m) \text{ in msec.}$$

$$g_m = 360 m^2 h (V - V_{N_a}) [d\alpha_m/dV - (d\alpha_m/dV + d\beta_m/dV) m] \tau_m \text{ in mmho/cm}^2$$

$$L_m = \tau_m/g_m \text{ in henries cm}^2$$

$$\tau_h = 1/(\alpha_h + \beta_h) \text{ in msec.}$$

$$g_h = 120 m^3 (V - V_{N_a}) [d\alpha_h/dV - (d\alpha_h/dV + d\beta_h/dV) h] \tau_h \text{ in mmho/cm}^2$$

$$L_h = \tau_h/g_h \text{ in henries cm}^2$$

$$\tau_n = 1/(\alpha_n + \beta_n) \text{ in msec.}$$

$$g_n = 144 n^3 (V - V_K) [d\alpha_n/dV - (d\alpha_n/dV + d\beta_n/dV) n] \tau_n \text{ in mmho/cm}^2$$

$$L_n = \tau_n/g_n \text{ in henries cm}^2$$

$$V_a = \text{axial wire potential (mv)}$$

$$g = \text{conductance in series with the membrane (mmho/cm}^2)$$

$$g_c = \text{critical value of } g \text{ which separates the region of stability from that of instability (mmho/cm}^2)$$

Considering now the second patch, the current I_2 in the equations is replaced by $(V_a - V_2)g$. When g is positive the Hodgkin-Huxley equations have only one singular point for each pair of values of g and V_a .³ The equations are linearized about this point, holding V_a constant, to give

$$d(\delta V)/dt = (\partial \dot{V}/\partial V) \delta V + (\partial \dot{V}/\partial m) \delta m + (\partial \dot{V}/\partial h) \delta h + (\partial \dot{V}/\partial n) \delta n \quad (5)$$

$$d(\delta m)/dt = (\partial \dot{m}/\partial V) \delta V + (\partial \dot{m}/\partial m) \delta m \quad (6)$$

$$d(\delta h)/dt = (\partial \dot{h}/\partial V) \delta V + (\partial \dot{h}/\partial h) \delta h \quad (7)$$

$$d(\delta n)/dt = (\partial \dot{n}/\partial V) \delta V + (\partial \dot{n}/\partial n) \delta n. \quad (8)$$

The parameters in equations (5) through (8) pertain to the second patch, although the subscript 2 has been omitted.

The elements of the matrix M , equations (1) and (3), are the partial derivatives in these equations evaluated at the singular point, and the characteristic equation, equation (4), is

$$g + F(\lambda) = 0, \quad (9)$$

where

$$F(\lambda) = g_\infty + \lambda C + g_m/(1 + \lambda\tau_m) + g_h/(1 + \lambda\tau_h) + g_n/(1 + \lambda\tau_n). \quad (10)$$

³ This is given by the intersection of the line $I = g(V_a - V)$ with the curve of steady-state current *versus* voltage.

The details of this derivation are given in the Appendix. The symbols used are given in the List of Symbols.

In Fig. 2, $F(\lambda)$ in mmho/cm^2 versus λ in msec^{-1} is shown for the resting potential. λ is generally complex but in Fig. 2 it is restricted to real values. There are three simple poles of $F(\lambda)$ at $-1/\tau_m$, $-1/\tau_h$, and $-1/\tau_n$. These are indicated by dashed lines crossing the abscissa. The real roots of the characteristic equation are given by the projections onto the λ axis of the intersections of the $F(\lambda)$ curve with

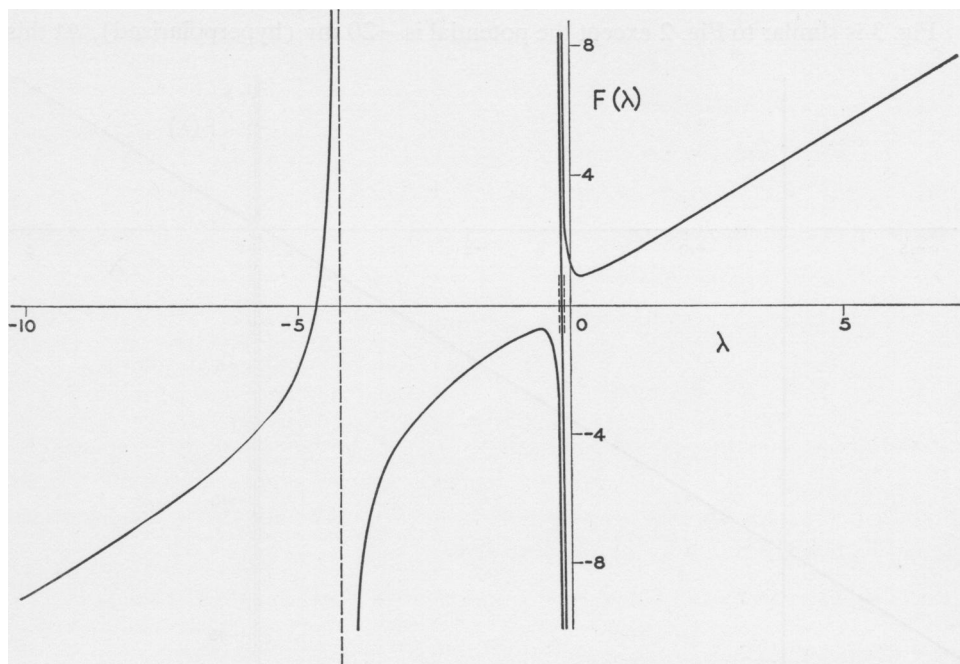


FIGURE 2 $F(\lambda)$ for real values of λ as calculated from the Hodgkin-Huxley equations, 6.3°C , at the resting potential. The characteristic equation, which describes the stability properties of the second patch, is $g + F(\lambda) = 0$, g being the series conductance. The real roots of this equation are given by the λ values of the intersections of $F(\lambda)$ with the horizontal line $F(\lambda) = -g$. Unstable behavior is possible when a root is positive. $F(\lambda)$ is in mmho/cm^2 , λ is in msec .

a horizontal line at ordinate $-g$. For $g > 0.812 \text{ mmho}/\text{cm}^2$ the four roots of the equation are real and negative. For $g < -0.897$ the four roots are real, and at least one is positive.

In the region $-0.897 < g < 0.812$ there are two negative real roots of the characteristic equation and a pair of complex conjugate roots,⁴ having either positive or negative real parts. When g is slightly larger than -0.897 , the real part

⁴ Since the coefficients in equation (9) are real, if a complex root satisfies the equation, so does its conjugate.

must be positive, while for g slightly less than 0.812, the real part is negative. It can be shown that between these two extremes there is a single value of conductance, the critical conductance, which gives rise to two complex roots which are pure imaginary numbers. However, the value of g_c cannot be determined from Fig. 2 in an easy manner.

The reciprocal of a positive real root of the characteristic equation (in this case for a series conductance less than -0.897 mmho/cm^2) is a time constant, as given in equation (2), associated with the growth of unstable perturbations.

Fig. 3 is similar to Fig. 2 except the potential is -20 mv (hyperpolarized). At this

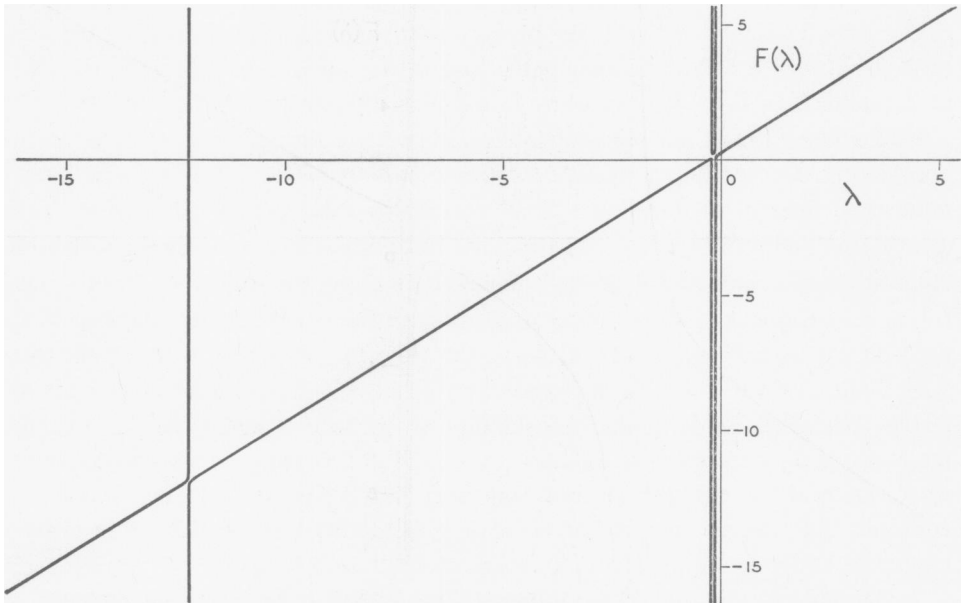


FIGURE 3 Same as Fig. 2 except the potential is -20 mv (hyperpolarized).

potential g_{Na} , g_K , g_m , g_h , and g_n are small and $F(\lambda)$ is essentially given by the first two terms in equation (10), except when λ lies in a region around one of the three vertical asymptotes. These asymptotes have λ values different from Fig. 2 since the time constants associated with m , h , and n are functions of voltage. The values of $F(\lambda)$ near the vertical asymptote on the right, given by $\lambda = -1/\tau_n$, have different signs in Figs. 2 and 3. This is because g_n is positive at the resting potential and negative at -20 mv .

From Fig. 3 we see that the values of conductance for which equation (9) has complex roots are narrowly bracketed and extend from minus the maximum of the branch of the $F(\lambda)$ curve second from the left to minus the minimum of the branch third from the left. It can be shown analytically that when these two extremes lie in the left half plane, such as in Fig. 3, the complex roots can have only

negative real parts. The critical conductance, given by $-F(0)$, is -0.296 mmho/cm². When the critical conductance is negative, as here, the second patch is stable for any positive g .

Thus far the analysis has been applied only to singular points, and has not been used to give the stability of the transient response of the second patch to a voltage clamp pulse. During a pulse a trajectory in the phase space of the variables V , m , h , and n is traced out by each patch. By solving the equations for a step change in membrane potential, the trajectory for the first patch, made stable by feedback, can be determined. This is also the exact, unperturbed mathematical solution for the second patch equations. However, we want to know if this intended response of the second patch is stable. If the phase point is moved a small distance from the trajectory, does it follow another path close to the original one, tending to return to it (stable), or does it move away to follow a different path (unstable)?

Kamenkov (1953) has defined stability for a finite time interval such as we are considering. Geometrically stated, a trajectory is stable at a given point over a finite time interval of duration τ if all perturbed phase points within some sufficiently small ellipsoid centered on the point in question at $t = t_0$ remain within the ellipsoid as its center moves through phase space along the trajectory, until at least $t = t_0 + \tau$. Kamenkov showed that if all roots of the characteristic equation at the point at $t = t_0$ have negative real parts, the trajectory is stable at that point over some finite interval $\tau > 0$. If any root has a positive real part, the trajectory is unstable. Therefore, to determine the stability of the second patch, we will examine the roots of the characteristic equation evaluated at operating points selected at 0.1 msec. intervals on the unperturbed trajectory. As before, V_0 can be treated as a constant. The degree or seriousness of any instability predicted by this analysis cannot be easily determined from the methods used in this paper.

In the calculations to follow, values of m , h , and n for -20 mv are used as initial conditions for each cathodal pulse. Compared with the resting potential, previous hyperpolarization of the Hodgkin-Huxley model results in larger peak inward currents and more of a tendency towards instability. Since the most powerful axons and the hyperpolarized axons are the most difficult to control experimentally, these initial conditions were chosen (Frankenhaeuser and Hodgkin, 1957; Cole and Moore, 1960).

During a step change of membrane potential, $F(\lambda)$ changes with time, starting from the curve shown in Fig. 3. Since the three poles of $F(\lambda)$ are negative, the three left branches of the $F(\lambda)$ curve always lie in the left half plane and give rise only to negative roots of the characteristic equation. Therefore, only the right-hand branch of the curve need be considered when looking for positive roots associated with instability.

At time zero, a step command pulse of 30 mv is applied to the input of the amplifier and instantaneously reproduced across both patches. In Fig. 4, the right-

hand branch of the $F(\lambda)$ curve is shown for times 0+, 0.2, 0.5, 1.0, 1.5, and 2.5 msec. At time zero the discontinuity in V produces two immediate changes in $F(\lambda)$. The λ value of the vertical asymptote of the curve changes discontinuously from -0.176 mmho/cm² (corresponding to $V = -20$ mv) to -0.317 mmho/cm² (corresponding to $V = 30$ mv) because of the discontinuous change in τ_n . Simultaneously, the asymptotic values of $F(\lambda)$ change from $-\infty$ to $+\infty$ because of the instantaneous change in sign of g_n associated with crossing the potassium equilibrium

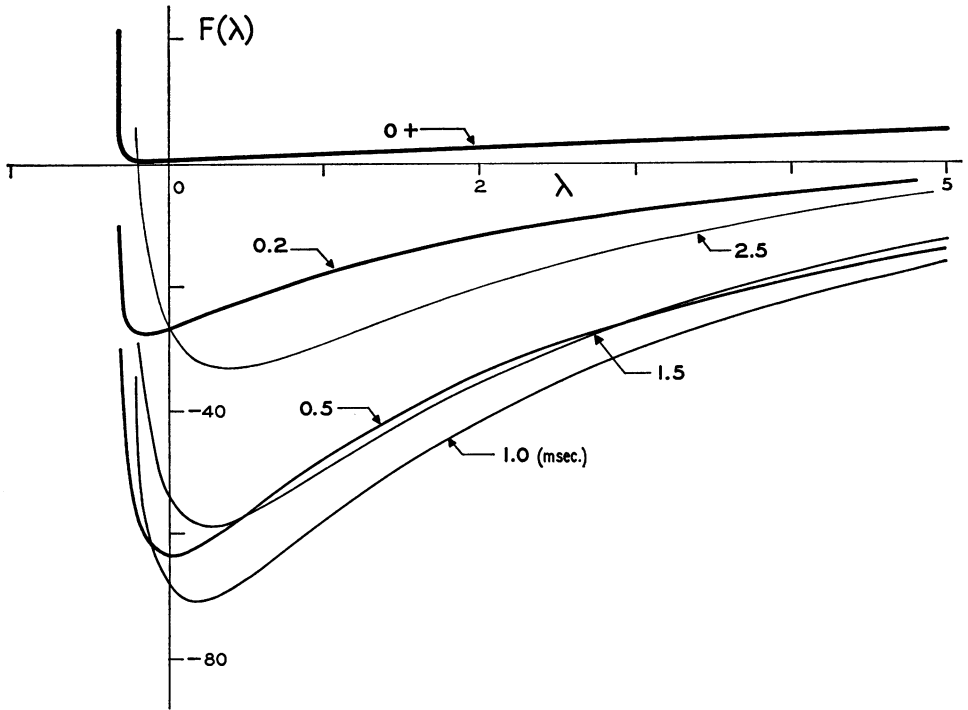


FIGURE 4 The right branch of the $F(\lambda)$ curve for various times following a cathodal step of 30 mv from the resting potential. The initial conditions were -20 mv. For times after 0+ the curve extends into the lower right quadrant, indicating that unstable behavior is possible if the series conductance is too small. The time constant in msec. associated with unstable behavior, positive λ , is the reciprocal of λ . Note the change in scale from the previous two figures.

potential V_K . After time zero, the curve changes continuously and finally approaches the steady state curve for 30 mv, not shown in the figure.

From the curve at 0.2 msec., a positive and a negative real root of the characteristic equation are obtained graphically for $g < 27$ mmho/cm², the critical conductance. Two negative real roots are obtained when g is between 27 and 28. For values of g between 28 and 60, the characteristic equation has two negative roots and a pair of complex roots. It can be shown that if the minimum in the

right hand branch of the $F(\lambda)$ curve lies in the left half plane, the complex roots have negative real parts.

At 1.0 msec. the minimum in the curve has moved into the right half plane and has a value of -71 mmho/cm². Therefore, a restricted range of values of the series conductance greater than 71 mmho/cm² will give rise to characteristic roots which are complex with positive real parts. There is no easy method for obtaining the value of the critical conductance from Fig. 4.

Thus, the curves shown in Fig. 4 give a clear picture of the time course of the positive real roots of the characteristic equation for a particular series conductance. However, these curves do not adequately describe the behavior of the characteristic equation when there is a region of conductances which give rise to complex roots with positive real parts. This region, when it exists, is particularly important because it includes the critical conductance. In this case, it is desirable to study the roots of the characteristic equation in a different manner.

NYQUIST CRITERION

The real and imaginary parts of any complex roots of equation (9) can be found by trial and error computations for each value of g selected. This complexity is necessary to get the numerical values of the roots. However, the value of the critical conductance can be obtained much more simply by applying a modification of the Nyquist criterion (Nyquist, 1932) to the generalized admittance calculated from the linearized Hodgkin-Huxley equations.

The Hodgkin-Huxley equations are linearized, as before, about either a singular point or a non-singular operating point. No substitution for membrane current is made. The Laplace transforms of these linearized equations (Churchill, 1944), using bars to indicate the transformed functions, are

$$\begin{aligned} p \bar{\delta V} &= (\partial \dot{V}/\partial V) \bar{\delta V} + (\partial \dot{V}/\partial m) \bar{\delta m} + (\partial \dot{V}/\partial h) \bar{\delta h} + (\partial \dot{V}/\partial n) \bar{\delta n} + (\partial \dot{V}/\partial I) \bar{\delta I} \\ p \bar{\delta m} &= (\partial \dot{m}/\partial V) \bar{\delta V} + (\partial \dot{m}/\partial m) \bar{\delta m} \\ p \bar{\delta h} &= (\partial \dot{h}/\partial V) \bar{\delta V} + (\partial \dot{h}/\partial h) \bar{\delta h} \\ p \bar{\delta n} &= (\partial \dot{n}/\partial V) \bar{\delta V} + (\partial \dot{n}/\partial n) \bar{\delta n}, \end{aligned}$$

where p is the transform variable. The generalized admittance, defined by

$$\bar{A}(p) = \bar{\delta I}/\bar{\delta V},$$

is obtained using Cramer's rule

$$\bar{A}(p) = g_\infty + pC + g_m/(1 + p\tau_m) + g_h/(1 + p\tau_h) + g_n/(1 + p\tau_n). \quad (11)$$

The admittance function is equal to $F(p)$ (cf. equations (35) and (36) of Hodgkin and Huxley (1952)).

The a.c. admittance $\bar{A}(j\omega)$, obtained when $j\omega$ replaces p , suggests the equivalent circuit

shown in Fig. 5.⁵ The membrane capacity is shunted by paths for sodium, potassium, and leakage currents. A conductance and inductance in series represents each of the linear approximations of the time dependent processes represented by *m*, *h*, and *n*. This is similar to the representation of a variable conductance with a single time constant given by Cole (1947). The conductances g_m , g_h , and g_n can be positive or negative, but the corresponding inductances must have the same sign since the time constants are positive.⁶ The sign of the conductance changes as the voltage moves from one side of the equilibrium potential of the ion in question to the other. For potentials between V_K and V_{Na} , the

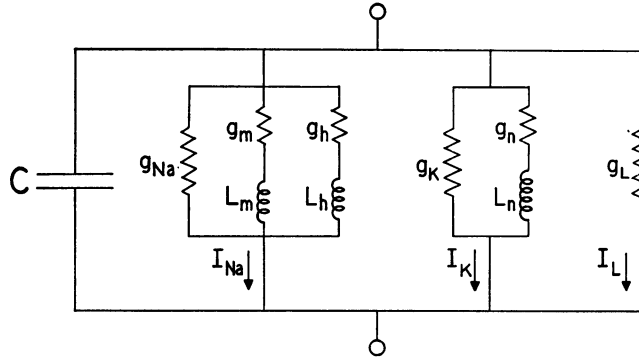


FIGURE 5 The equivalent A.C. circuit for the linearized Hodgkin-Huxley membrane. The infinite frequency conductances of sodium and potassium, g_{Na} and g_K , are shunted by series conductance and inductance elements representing *m*, *h*, and *n*. The elements for sodium activation, g_m and L_m , are both negative, and are responsible for the tendency towards instability present during voltage clamp pulses.

sodium activation process (*m*) gives a negative conductance (g_m), while sodium inactivation (*h*) and potassium activation (*n*) give positive conductances (g_h and g_n). It is this negative conductance associated with sodium activation that can cause instability in the Hodgkin-Huxley axon during a voltage clamp pulse.

The generalized admittance may now be used to represent each membrane in the two patch model. A small perturbing voltage $\delta \bar{V}_a$ is applied to the axial wire. The perturbation of the second patch current is

$$\bar{A}(p) \delta \bar{V} = (\delta \bar{V}_a - \delta \bar{V})g.$$

This expression can be rearranged to give an overall transfer function from the wire to the second patch

$$\delta \bar{V} / \delta \bar{V}_a = g / [g + \bar{A}(p)]. \quad (12)$$

Although there is no negative feedback from the potential of the second patch

⁵ j is identically equal to $\sqrt{-1}$ and ω is equal to 2π times the frequency.

⁶ A negative conductance and inductance in series are formally equivalent to a negative conductance in parallel with a positive capacitance and positive conductance in series. Thus, the terms inductive and capacitive reactances can be used to describe these time dependent, ionic processes.

to the axial wire, the transfer function, equation (12), is similar to those developed in the theory of servomechanisms, and the Nyquist criterion can be employed to determine the stability of the second patch. The reader interested in the details of the Nyquist criterion may refer to one of the numerous books on the subject, such as James, Nichols, and Philips (1947) or Truxal (1955). The appropriate analysis shows that the second patch is stable if the denominator of the transfer function given by equation (12) has no zeros with positive real parts (compare with equation (9)). The essential result is that the critical conductance is given by the negative value of the intersection farthest left which the A.C. admittance locus makes with the real axis. This intersection will be referred to as the "left" intersection.

The A.C. admittance locus at the resting potential, as calculated from equation (11), with and without a static capacity of $1\mu\text{f}/\text{cm}^2$, is shown in Fig. 6a. The admittance locus of a constant conductance in parallel with a static capacity is a

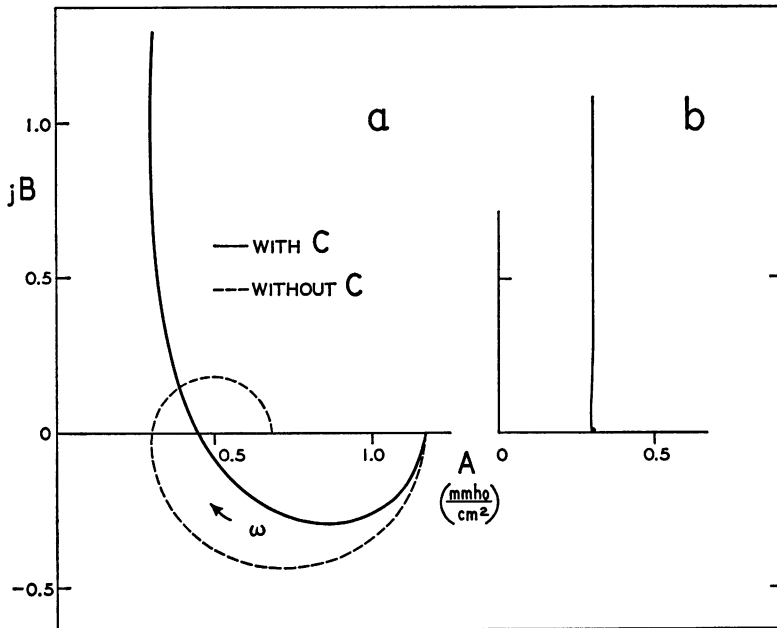


FIGURE 6 (a) The admittance of the Hodgkin-Huxley membrane at 6.3° for the resting potential. The susceptance (ordinate) and conductance (abscissa) are in mmho/cm^2 . The dashed curve is the ionic part; the heavy curve includes a parallel static capacity of $1\mu\text{f}/\text{cm}^2$. The arrow shows the direction of increasing frequency. The left intersection of the admittance locus with the abscissa gives the negative value of the critical conductance. A series conductance greater than the critical value results in stable behavior, while a smaller conductance can cause unstable behavior. The ionic admittance is essentially the same as given by Cole (1955) in Fig. 16. (b) Similar to Fig. 6a for a potential of -20 mv. At this potential the sodium and potassium conductances are negligible, so the ionic conductance is mostly leakage.

vertical, straight line. The curved shape of the Hodgkin-Huxley locus is caused by the reactances associated with m , h , and n . The critical conductance is -0.446 mmho/cm² which means the second patch is stable at the resting potential for any positive g .

In Fig. 6*b* the admittance for -20 mv is shown. As in Fig. 3, the membrane is seen to approximate a constant conductance and capacity in parallel.

At time zero a cathodal step of 30 mv with respect to the resting potential is applied to the hyperpolarized membrane model. Admittances for times 0+, 0.2, 0.5, 1.0, 1.5, and 2.5 msec. are shown in Fig. 7. At time 0+ the admittance has

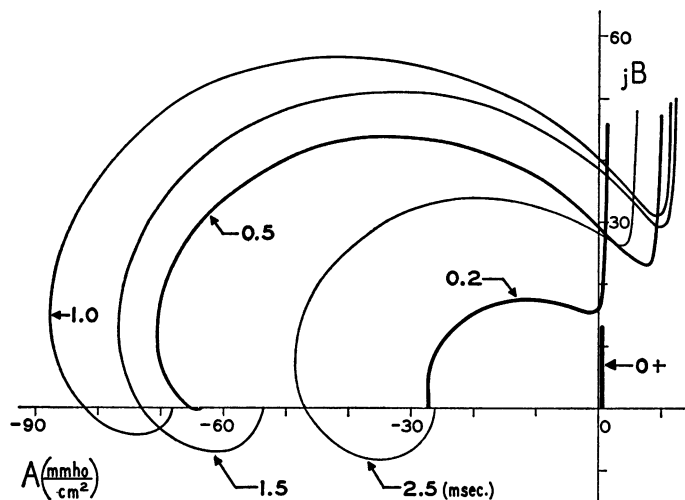


FIGURE 7 Admittances for various times following a cathodal step from -20 mv to 30 mv. The scale is different from Fig. 6. The critical conductance goes through a maximum at 1 msec. with a value of 82 mmho/cm².

changed slightly from that shown in Fig. 6*b*. At 0.2 msec. the curve has enlarged and moved to the left. The curve continues in this direction until at 1 msec. it turns and starts towards the right. For a long enough pulse the admittance curve would reach the steady state curve for 30 mv, not shown in the figure.

The negative of the critical conductance, $-g_c$, can be read from the left intersection of the admittance locus with the real axis. For times 0+ and 0.2 msec. these intersections occur at zero frequency and, as was seen in Fig. 4, the critical conductance gives rise only to real roots of the characteristic equation. At the later times the left intersection occurs at a frequency greater than zero, and the critical conductance gives rise to two imaginary roots. The 1 msec. locus shows a peak value of critical conductance of 82 mmho/cm². Conductances between -68 and -82 mmho/cm² are encircled twice by the complete Nyquist plot, showing that two roots have positive real parts. Unfortunately, these admittance diagrams do not

readily give information on the magnitudes of the real parts of the roots of the characteristic equation.

Curves of critical conductance *versus* time following step depolarizations of 20, 30, 40, and 50 mv are shown in Fig. 8. (The values of critical conductance were interpolated from admittance locus plots such as those shown in Fig. 7.) During a given step depolarization, the second patch is stable if the series conductance is greater than the maximum critical conductance calculated for that voltage.

A summary of the critical conductance calculations is given in Fig. 9 in the curve labeled Nyquist. The maxima of the curves of critical conductance *versus*

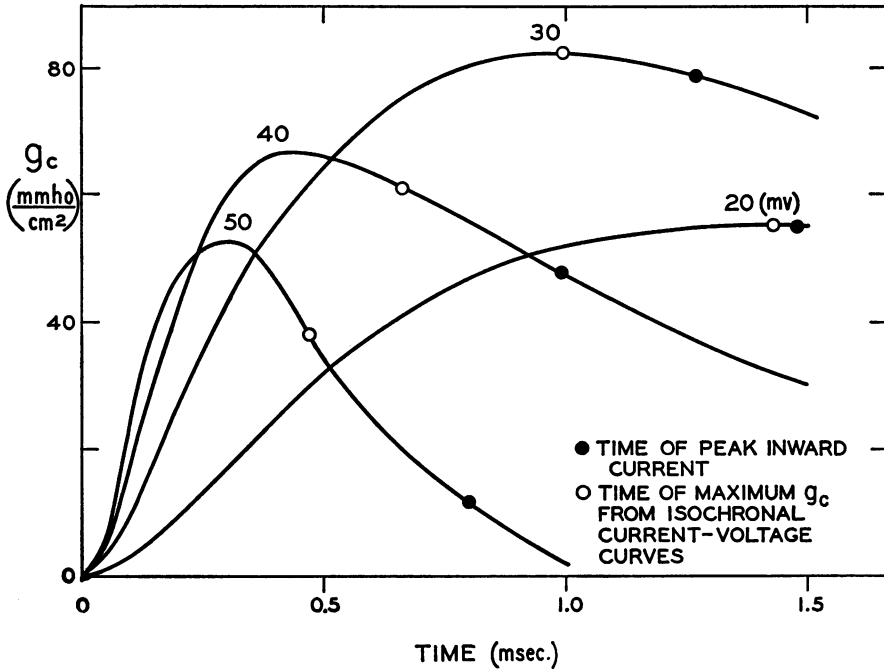


FIGURE 8 Critical conductance in mmho/cm² *versus* time following step depolarizations of 20, 30, 40, and 50 mv. The peaks in the curves occur earlier for the larger depolarizations, and precede the occurrence of peak inward current and maximum isochronal g_c . Each curve separates a region of conductance values associated with stable behavior (above) from a region capable of causing unstable behavior (below).

time, such as shown in Fig. 8, are plotted as a function of clamping potential. At 29 mv the maximum critical conductance has a peak value of 83 mmho/cm².

QUASI-STEADY STATE CHARACTERISTIC

One of the purposes of this study was to develop a criterion for deciding experimentally whether stable space clamp behavior could be expected from a given length of fresh axon. Cole and Moore (1960, Appendix D) suggested using the

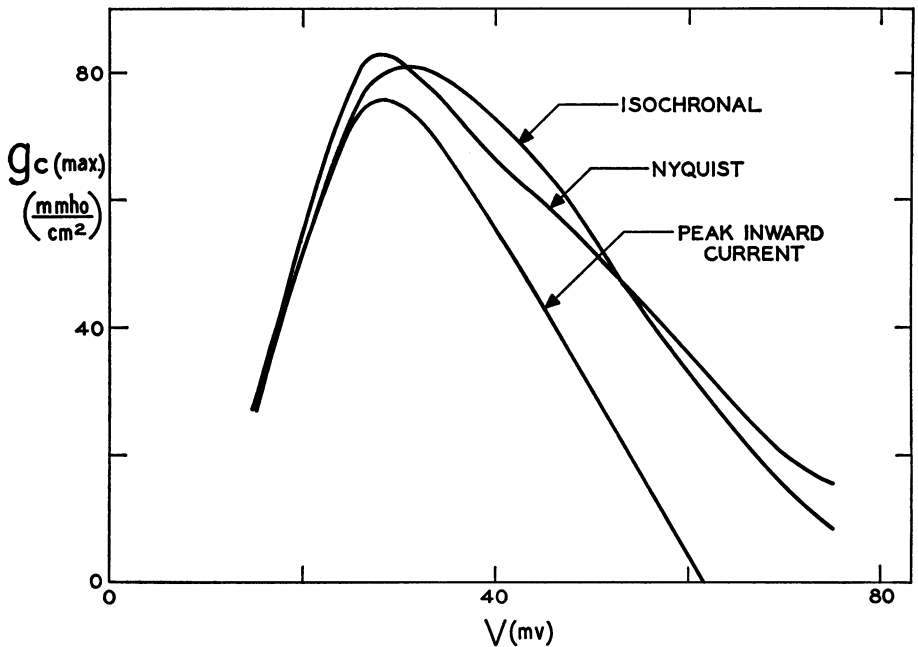


FIGURE 9 Maximum critical conductance for each voltage step calculated by three methods. The curve labeled Nyquist gives the values obtained from the Nyquist criterion. The peak inward current curve is determined on the assumption that the peak inward current *versus* voltage curve for the membrane is a quasi-steady state characteristic. See text for details on isochronal curve. All calculations were made on the Hodgkin-Huxley equations, 6.3°C, with initial conditions of -20 mv (hyperpolarization).

experimentally obtained peak inward current *versus* voltage curve as a quasi-steady state characteristic of ionic conductance. At a given voltage, the critical conductance of a membrane having this characteristic is equal to the negative slope of the curve. To examine the validity of this quasi-steady state approximation for the Hodgkin-Huxley equations, we calculated the values of peak inward current from the equations. The critical conductances, obtained from interpolations of these currents, are shown in Fig. 9 in the curve labeled peak inward current. This curve has a maximum value of 76 mmho/cm² and is sufficiently similar to the curve labeled Nyquist to justify the approximation of Cole and Moore and of Cole (1961), at least with respect to the Hodgkin-Huxley axon.

Somewhat along the same line, the curves of current *versus* voltage at different times can be used as quasi-steady state characteristics, from which a critical conductance for each voltage at each time can be obtained. The maximum values in time of these critical conductances, each one calculated from pairs of calculations made 0.01 mv apart, are shown in the curve labeled isochronal.

The three curves shown in Fig. 9 are quite similar. However, the times as-

sociated with peak inward current, maximum Nyquist critical conductance, and maximum isochronal critical conductance are different, as seen in Fig. 8. These differences are more pronounced at the larger depolarizations.

DISCUSSION

The mathematical analysis presented thus far should be useful in two ways to the physiologist interested in voltage clamp experiments on squid giant axons. First, it provides an analytical method which, when applied to the Hodgkin-Huxley equations, defines a region of values of the series conductance for which instability can be expected in an indefinitely long, uniform axon. Second, the correlation in the Hodgkin-Huxley equations of the maximum critical conductance with both the negative slope of the peak inward current *versus* voltage curve and the largest negative slope of the isochronal inward current *versus* voltage curves gives some basis for assuming the same correlation to exist in the nerves used in experiments at the present time. It must be strongly emphasized that the Hodgkin-Huxley equations represent an empirical description of the voltage clamp currents, and the conclusions derived from them here are entirely independent of any physical interpretations given to any symbols other than I and V .

Although the present analysis has been restricted primarily to a study of space clamp stability, the mathematical methods employed can be directly applied to the investigation of other stability phenomena. The most general case would be an arbitrary voltage source $V_a(t)$ connected to the membrane through a series conductance g . As an example (see FitzHugh, 1961), the response of a uniform patch of membrane to constant current pulses can be explored by using step changes of V_a , and then allowing g to approach zero and V_a to approach infinity in such a way as to make gV_a approach the constant current value. For an indefinitely long current pulse, an unstable singular point for $g = 0$ at the appropriate point on the steady-state current *versus* voltage curve implies a response of an infinite train of action potentials. A stable singular point implies a response of at most a finite number of action potentials.

Admittances in the entire frequency range including zero cycles per second have been calculated from the Hodgkin-Huxley equations. The low frequencies might appear irrelevant, since the times associated with the duration of voltage clamp pulses and membrane transients are usually in milliseconds. However, these frequencies are needed to complete the closed curve in the admittance plane which is used in the Nyquist criterion. In fact, the point $(-g_0, 0)$ on the admittance curve occurs in this frequency range, usually between 0 and 100 cycles per second for 6.3°C . Although these low frequency admittances can have no experimental realization during the early part of a voltage clamp pulse, they are nonetheless helpful in locating regions of conductance for which the characteristic equation has roots with positive real parts.

When the series conductance is close in value to the critical conductance, and the point $(-g_0, 0)$ on the admittance locus occurs for a frequency greater than zero, small perturbations oscillate at about that same frequency. These oscillations decrease or increase in magnitude, depending respectively on whether $g > g_0$ or $g < g_0$. Some examples of such oscillations are given by Huxley (1959). Similarly, there is a rough agreement between the frequencies of oscillation reported by Tasaki *et al.* (Tasaki and Bak, 1958; Tasaki and Spyropoulos, 1958) and the values which we have calculated but shall not present in detail.

The two patch model gives a picture of the stability properties of membrane at the control point and of membrane some distance away. The first patch is always controlled by the high gain amplifier, while the second patch is controlled if $g > g_0$ and uncontrolled if $g < g_0$. Experimentally, an area of membrane near the control point might be expected to have intermediate stability. This can be represented by a linked two patch model. A conductance G , representing the longitudinal conductance of the axoplasm between the patches, is connected between the two points marked V_1 and V_2 in Fig. 1. When the appropriate analysis is carried out, the expression analogous to the denominator of equation (12) is found to be approximately

$$\bar{A}(p) + 2G + g = 0.$$

The Nyquist criterion indicates that the effective series conductance to the second patch is $2G + g$, instead of g . When the second patch represents membrane far from the control point, G approaches zero which agrees with the unlinked two patch model. As membrane closer to the control point is simulated by the second patch, G becomes larger and stability is more easily maintained.

The Nyquist criterion can be applied to networks more detailed than the two patch model. In such networks the membrane properties are represented by the A.C. admittance. However, the admittance loci which we have calculated from the Hodgkin-Huxley equations are applicable only to parts of the membrane which have followed a step change in potential prior to the time of calculation. Admittance loci for parts of the membrane which have followed a different time course must be computed as needed. One of us (RF) has begun to analyze the linear cable model of uniform nerve to determine the conditions necessary for stability during a step voltage pulse. Perfect seals which block longitudinal current flow are used for boundary conditions at each end of the clamped nerve. Stability for an indefinitely long length of clamped nerve requires the same minimum series conductance as the two patch model. As the length is shortened, this critical value is decreased until, for an infinitesimal length, the nerve is always stable. Mathematically, the effect of having a finite length is equivalent with respect to stability to the addition of a conductance in parallel with the series conductance and having a value inversely proportional to length squared. This conductance acts in the same way as the term $2G$ in the linked two patch model and is negligible when the length

of nerve is more than several space constants. As mentioned previously, the space constant of a squid giant axon with an axial electrode is less than 1 mm.

When instability is predicted by the Nyquist criterion, the admittance locus does not give information on the electrical events which will actually occur. The amount small perturbations grow will depend on the magnitude of the perturbations, the magnitude of the positive real parts of the unstable roots, and the length of time the system is unstable. In addition, an unstable solution may enter a region of phase space in which the approximation of the original linearization of the differential equations is poor. If this happens, the nonlinearities become important, and the actual solutions must be obtained from the complete nonlinear equations. Some investigations along these lines have been completed by Taylor *et al.* (Taylor and FitzHugh, 1959; Taylor, Moore, and Cole, 1960) and by Cole (1961).

The remainder of the discussion will be devoted to a consideration of the changes in the stability properties of the membrane produced by changes in certain terms in equations (11) and (12).

Capacity. The effect of membrane capacity on the stability properties can be seen graphically from a plot of the ionic admittance. A static capacity added in parallel raises the curve of the ionic admittance by an amount ωC at each point, as shown in Fig. 6. This decreases the critical conductance in those cases where the left intercept does not occur at zero frequency. However, in no case does the critical conductance become less than the value given by the negative of the zero frequency admittance.

The static capacity may be replaced by a polarization element with an admittance $(j\omega C)^{\alpha}$ as considered by Curtis and Cole (1938). From their data we selected a phase angle of 75° ($\alpha = 5/6$) and a capacity of $1\mu\text{f}/\text{cm}^2$ at 1 kilocycle as representative of the squid giant axon. When in parallel with the ionic admittance, this element, represented by a straight line in the admittance plane with slope $\tan(\alpha\pi/2)$, shifts each point on the ionic admittance both up and to the right.

The following values of critical conductance are obtained at 1 msec. for a 30 mv depolarization (see Fig. 7): (1) 82.4 mmho/cm² without a parallel capacity, (2) 82.1 mmho/cm² with a parallel capacity of $1\mu\text{f}/\text{cm}^2$, and (3) 81.7 mmho/cm² with the parallel polarization element. Differences between these values are small.

Temperature. The effect of temperature on the critical conductance can also be seen graphically. In the Hodgkin-Huxley equations, an increase of temperature decreases the time constants of m , h , and n with a Q_{10} of 3. At temperature T , $\tau_{6.3}^{\circ} = \tau_T \Phi_T$, $\Phi_T = 3^{(T-6.3)/10}$, and equation (11) becomes

$$\begin{aligned} \bar{A}(j\omega) = & g_{\infty} + j(\omega/\Phi_T)\Phi_T C + g_m/[1 + j(\omega/\Phi_T)\tau_m] \\ & + g_h/[1 + j(\omega/\Phi_T)\tau_h] + g_n/[1 + j(\omega/\Phi_T)\tau_n], \end{aligned}$$

where the τ 's are appropriate for 6.3°C. A change in temperature produces a change in the critical conductance equivalent to that produced by multiplying the mem-

brane capacity by ϕ_T . This causes the axon to have more of a tendency for unstable behavior at lower temperature.

On the other hand, Moore (1958) has shown that raising the temperature from 5°C to 25°C increases the peak sodium conductance and steady-state potassium conductance by 4 per cent per degree relative to 15°C. If these effects are interpreted as equivalent changes of \bar{g}_{Na} and \bar{g}_K , the ionic admittance would spread in all directions from the origin as the temperature was increased, and the critical conductance would increase. On the basis of rough calculations, these two opposite effects of temperature combine to give a net increase in critical conductance with an increase in temperature.

Electrode Polarizability. The assumption that the series conductance is constant and frequency independent is not strictly valid under the usual experimental conditions. The element included in the series conductance which probably deviates most from being constant is the axial electrode. If the admittance of this is represented by a polarization term of the form $(pC_e)^x$, we can replace g in equation (12) by $g(pC_e)^x / [g + (pC_e)^x]$. This change results in predicted instability for many cases where the left intersection of the admittance locus with the real axis occurs in the left half of the admittance plane and for all cases where the zero frequency admittance is also in the left half plane. On this basis it would seem impossible to clamp adequately any good axon. Rough calculations using a value of $\frac{1}{2}$ for x and a value for C_e appropriate for the electrodes used in this laboratory indicate that the time constant associated with the instability is large if g is much larger than g_c . Thus, the growth of unstable perturbations might be sufficiently small to prevent their being serious. At any rate, the electrode polarizability must be considered as a factor which tends to make the system unstable.

CONCLUSIONS

Application of the Nyquist criterion to the A.C. admittance of the Hodgkin-Huxley equations has been successful in giving an analytical basis both for unstable axon behavior during voltage clamp experiments and for the computed results on the two patch model. The axial current electrode, axoplasm, and small layer of sea water surrounding the nerve, all in series, should have a combined conductance greater than 83 mmho/cm²—or resistance less than 12 ohm cm²—to insure stability for all pulses preceded by a 20 mv hyperpolarization. To extend this analysis to nerves presently being studied experimentally, either an adequate mathematical description of them must be available or certain assumptions must be made. The simplest assumption, which we showed was reasonable for the Hodgkin-Huxley axon, is to take the negative of the slope of the peak inward current *versus* voltage curve as an approximation to the critical conductance which would be determined from more exact calculations. The average of the peak value of this quantity for the squid giant axons studied in this Laboratory is 250 mmho/cm², with some axons

giving values up to 500 mmho/cm² (Cole and Moore, 1960). As the calculated conductance of the axoplasm plus the small, external layer of sea water does not exceed 500 mmho/cm², perfect electrodes would give a series conductance close in value to the critical conductance. As non-uniformities (Taylor, Moore, and Cole, 1960) and electrode polarization make stable control more difficult, one must entertain the rather pessimistic view, based on the above assumption, that adequate voltage control over a few millimeters of "hot" axon might be impossible. Such space clamp failure would necessitate the use of techniques for measuring membrane current through a small, relatively uniform area about the control point.

We are grateful to Dr. Robert E. Taylor for many helpful suggestions and criticisms. Most of the calculations of $F(\lambda)$ and the a.c. admittance were done on an IBM 650 digital computer at the National Institutes of Health, and we are indebted to Mr. John Witmer for assistance in using the computer.

A preliminary report has been made (Chandler, 1961).

Received for publication, September 5, 1961.

REFERENCES

- ADAMS, E. P., 1957, *Smithsonian Mathematical Formulae and Tables of Elliptic Functions*, Washington, D. C., Smithsonian Institution.
- ANDRONOW, A. A., and CHAIKIN, C. E., 1949, *Theory of Oscillations*, Princeton, Princeton University Press.
- BELLMAN, R., 1953, *Stability Theory of Differential Equations*, New York, McGraw-Hill Book Co.
- CHANDLER, W. K., 1961, Stability of the Hodgkin-Huxley axon equations, *Abstr., Biophysic. Soc.*, FC4.
- CHURCHILL, R. V., 1944, *Modern Operational Mathematics in Engineering*, New York, McGraw-Hill Book Co.
- COLE, K. S., 1947, Four lectures on biophysics, Institute of Biophysics, University of Brazil.
- COLE, K. S., 1949, Dynamic electrical characteristics of the squid axon membrane, *Arch. Sc. Physiol.*, 3, 253.
- COLE, K. S., 1955, Ions, potentials, and the nerve impulse, in *Electrochemistry in Biology and Medicine*, (T. Shedlovsky, editor), New York, John Wiley and Sons, 134.
- COLE, K. S., 1961, An analysis of the membrane potential along a clamped squid axon, *Biophysic. J.*, 1, 401.
- COLE, K. S., and MOORE, J. W., 1960, Ionic current measurements in the squid giant axon membrane, *J. Gen. Physiol.*, 44, 123.
- CURTIS, H. J., and COLE, K. S., 1938, Transverse electric impedance of the squid giant axon, *J. Gen. Physiol.*, 21, 757.
- FITZHUGH, R., 1961, Impulses and physiological states in theoretical models of nerve membrane, *Biophysic. J.*, 1, 445.
- FRANKENHAEUSER, B., and HODGKIN, A. L., 1957, The action of calcium on the electrical properties of squid axons, *J. Physiol.*, 137, 217.
- HODGKIN, A. L., and HUXLEY, A. F., 1952, A quantitative description of membrane current and its application to conduction and excitation in nerve, *J. Physiol.*, 117, 500.
- HODGKIN, A. L., HUXLEY, A. F., and KATZ, B., 1952, Measurement of current-voltage relations in the membrane of the giant axon of *Loligo*, *J. Physiol.*, 116, 424.
- HUXLEY, A. F., 1959, Ion movements during nerve activity, *Ann. New York Acad. Sc.*, 81, 221.

- JAMES, H. M., NICHOLS, N. B., and PHILLIPS, R. S., 1947, *Theory of Servomechanisms*, New York, McGraw-Hill Book Co.
- KAMENKOV, G. V., 1953, On the stability of motion in a finite time interval, *Prikl. Mat. Mekh.*, **17**, 529.
- LEFSCHETZ, S., 1957, *Differential Equations: Geometric Theory*, New York, Interscience Publishers, Inc.
- MINORSKY, N., 1947, *Introduction to Non-Linear Mechanics*, Ann Arbor, J. W. Edwards.
- MOORE, J. W., 1958, Temperature and drug effects on squid axon membrane ion conductances, *Fed. Proc.*, **17**, 113.
- NEMYTSKII, V. V., and STEPANOV, V. V., 1960, *Qualitative Theory of Differential Equations*, Princeton, Princeton University Press.
- NYQUIST, H., 1932, Regeneration theory, *Bell System Techn. J.*, **11**, 126.
- TASAKI, I., and BAK, A. F., 1958, Discrete threshold and repetitive responses in the squid axon under "voltage-clamp," *Am. J. Physiol.*, **193**, 301.
- TASAKI, I., and SPYROPOULOS, C. S., 1958, Nonuniform response in the squid axon membrane under "voltage-clamp," *Am. J. Physiol.*, **193**, 309.
- TAYLOR, R. E., and FITZHUGH, R., 1959, A source of anomalous current patterns in the "voltage clamped" squid axon, *Abstr., Biophysic. Soc.*, G6.
- TAYLOR, R. E., MOORE, J. W., and COLE, K. S., 1960, Analysis of certain errors in squid axon voltage clamp measurements, *Biophysic. J.*, **1**, 161.
- TRUXAL, J. G., 1955, *Automatic Feedback Control System Synthesis*, New York, McGraw-Hill Book Co.

APPENDIX

Starting with the Hodgkin-Huxley equations for the second patch and omitting the subscript 2 we have

$$\begin{aligned}\dot{V} &= (V_a - V)g/C = \bar{g}_{Na}m^3h(V - V_{Na})/C - \bar{g}_Kn^4(V - V_K)/C - \bar{g}_L(V - V_L)/C \\ \dot{m} &= \alpha_m(1 - m) - \beta_m m \\ \dot{h} &= \alpha_h(1 - h) - \beta_h h \\ \dot{n} &= \alpha_n(1 - n) - \beta_n n.\end{aligned}$$

The coefficients in equations (5) through (8) are

$$\begin{aligned}m_{11} &= (\partial \dot{V} / \partial V) = -g/C - \bar{g}_{Na}m^3h/C - \bar{g}_Kn^4/C - \bar{g}_L/C \\ m_{12} &= (\partial \dot{V} / \partial m) = -3\bar{g}_{Na}m^2h(V - V_{Na})/C \\ m_{13} &= (\partial \dot{V} / \partial h) = -\bar{g}_{Na}m^3(V - V_{Na})/C \\ m_{14} &= (\partial \dot{V} / \partial n) = -4\bar{g}_Kn^3(V - V_K)/C \\ m_{21} &= (\partial \dot{m} / \partial V) = (1 - m)(d\alpha_m/dV) - m(d\beta_m/dV) \\ m_{22} &= (\partial \dot{m} / \partial m) = -(\alpha_m + \beta_m) \\ m_{31} &= (\partial \dot{h} / \partial V) = (1 - h)(d\alpha_h/dV) - h(d\beta_h/dV) \\ m_{33} &= (\partial \dot{h} / \partial h) = -(\alpha_h + \beta_h) \\ m_{41} &= (\partial \dot{n} / \partial V) = (1 - n)(d\alpha_n/dV) - n(d\beta_n/dV) \\ m_{44} &= (\partial \dot{n} / \partial n) = -(\alpha_n + \beta_n).\end{aligned}$$

In matrix notation we can write (5) – (8) as

$$\begin{pmatrix} d(\delta V)/dt \\ d(\delta m)/dt \\ d(\delta h)/dt \\ d(\delta n)/dt \end{pmatrix} = \begin{pmatrix} m_{11} & m_{12} & m_{13} & m_{14} \\ m_{21} & m_{22} & 0 & 0 \\ m_{31} & 0 & m_{33} & 0 \\ m_{41} & 0 & 0 & m_{44} \end{pmatrix} \begin{pmatrix} \delta V \\ \delta m \\ \delta h \\ \delta n \end{pmatrix}.$$

We assume a solution of the form

$$\delta V = a_v \exp(\lambda t)$$

$$\delta m = a_m \exp(\lambda t)$$

$$\delta h = a_h \exp(\lambda t)$$

$$\delta n = a_n \exp(\lambda t),$$

and get

$$\lambda \exp(\lambda t) \begin{pmatrix} a_v \\ a_m \\ a_h \\ a_n \end{pmatrix} = \exp(\lambda t) \begin{pmatrix} m_{11} & m_{12} & m_{13} & m_{14} \\ m_{21} & m_{22} & 0 & 0 \\ m_{31} & 0 & m_{33} & 0 \\ m_{41} & 0 & 0 & m_{44} \end{pmatrix} \begin{pmatrix} a_v \\ a_m \\ a_h \\ a_n \end{pmatrix},$$

which reduces to

$$\begin{pmatrix} m_{11} - \lambda & m_{12} & m_{13} & m_{14} \\ m_{21} & m_{22} - \lambda & 0 & 0 \\ m_{31} & 0 & m_{33} - \lambda & 0 \\ m_{41} & 0 & 0 & m_{44} - \lambda \end{pmatrix} \begin{pmatrix} a_v \\ a_m \\ a_h \\ a_n \end{pmatrix} = 0.$$

The a 's are different from zero only if the determinant

$$\begin{vmatrix} m_{11} - \lambda & m_{12} & m_{13} & m_{14} \\ m_{21} & m_{22} - \lambda & 0 & 0 \\ m_{31} & 0 & m_{33} - \lambda & 0 \\ m_{41} & 0 & 0 & m_{44} - \lambda \end{vmatrix} = 0.$$

Evaluating this we get

$$(m_{11} - \lambda)(m_{22} - \lambda)(m_{33} - \lambda)(m_{44} - \lambda) - m_{12}m_{21}(m_{33} - \lambda)(m_{44} - \lambda) \\ - m_{13}m_{31}(m_{22} - \lambda)(m_{44} - \lambda) - m_{14}m_{41}(m_{22} - \lambda)(m_{33} - \lambda) = 0,$$

which gives

$$-m_{11}C + \lambda C + (m_{12}m_{21}C/m_{22})/(1 - \lambda/m_{22}) \\ + (m_{13}m_{31}C/m_{33})/(1 - \lambda/m_{33}) + (m_{14}m_{41}C/m_{44})/(1 - \lambda/m_{44}) = 0,$$

the same as equation (9).